The effective modification of spinel inclusions by Ca treatment in LCAK steel.

This paper postulates the mechanisms of spinel formation in LCAK steel produced via the EAF route. The effective modification of solid spinel inclusions into liquid inclusions by Ca treatment is also demonstrated.

Eugene B. Pretorious, *Manager, steelmaking technology, Nucor Steel-Berkeley*
Helmut G. Oltmann, *Meltshop metallurgist, Nucor Steel-Berkeley*
Thomas Cash, *Melt cast mananger, Nucor Steel-Arkansas*

The Effective Modification of Spinel Inclusions by Ca Treatment in LCAK Steel

This paper was granted the 2010 AIST Ladle and Secondary Refining Award for Best Paper, and will therefore automatically be considered for the 2011 Hunt-Kelly Outstanding Paper Award.

Spinel inclusions have for a long time been considered to be very harmful to castability and product quality. The following quotations demonstrate the general view on spinel inclusions:

- The dirty word — spinels!"[1]
- "Spinel is known as one of the most harmful non-metallic inclusions in steel."[2]
- "Catastrophic plugging of calcium-treated steels seems to correlate with the presence of spinel."[3]
- "Spinel, just like alumina inclusions, deteriorates the final quality of steel products because it has a high melting point and exists as a C-type inclusion, which is not plastically deformed and evenly dispersed. It also induces nozzle clogging, which decreases productivity and process effectiveness."[4]

The review papers by Larry Frank give an excellent overview of the impact of non-metallic inclusions on castability.[1] Spinel inclusions are specifically singled out as being very harmful in terms of clogging at the caster and surface quality of the final product.

While there is absolute consensus in the literature that spinel inclusions will cause clogging at the caster, there is some difference of opinion on whether spinel inclusions can be modified to liquid inclusions by calcium treatment. Some papers suggest that the modification of spinels by calcium would be less effective than the modification of pure alumina, and that prevention or suppression of spinel inclusions should be pursued.[1,5] This is indeed the practice at some plants producing IF steel via the RH degasser route, where fairly oxidizing ladle slags (> 6% FeO) are targeted to suppress the formation of spinels. Other operations add Al as late as possible to the heat to minimize spinel formation.[3] However, more recent work indicates that, under very reducing conditions (steel and slag), some spinel modification by calcium treatment is possible, and it is even suggested that the modification of spinel inclusions by calcium treatment would be easier than alumina inclusions.[3,6–8] The work reported in this paper is consistent with these findings, and it will show that complete modification of spinel inclusions by calcium is possible. This work will further show that effective spinel modification actually involves two steps: (1) modifying the spinels with calcium and (2) keeping them modified.

This paper postulates the mechanisms of spinel formation in LCAK steel produced via the EAF route. The effective modification of solid spinel inclusions into liquid inclusions by Ca treatment is also demonstrated.

A scanning electron microscope (SEM) with automated feature analysis was utilized to evaluate the inclusions in metal samples from many heats. These samples were taken at various stages of a heat, i.e., before Ca treatment, after Ca treatment, in the tundish, and from the final strip product. The results reported in this paper are representative of hundreds of metal samples, and the inclusion modifications demonstrated are consistent from heat to heat. This paper will postulate the mechanisms of spinel formation in LCAK steel produced via the EAF route and demonstrate the effective modification of the solid spinel inclusions into liquid inclusions by Ca treatment. The theoretical and practical aspects of spinel modification will be discussed, and the requirements for effective modification will be elucidated.

Authors

Eugene B. Pretorius (left), manager — steelmaking technology, and **Helmut G. Oltmann** (center), meltshop metallurgist, Nucor Steel–Berkeley, Mt. Pleasant, S.C. (eugene.pretorius@nucor.com, helmut.oltmann@nucor.com); and **Thomas Cash** (right), melt cast manager, Nucor Steel–Arkansas, Armorel, Ark. (thomas.cash@nucor.com)



Table 1

Typical Inclusion Data as Reported During AFA Analysis

Inclusion class	Avg. dia. (µm)	%Mg	%Al	%Si	%S	%Ca	%Ti	%Mn
Alumina	3.41	0	98.2	0	0.7	1.1	0	0
Lo-Mg alumina	1.36	14.7	75.8	0	2.8	3.8	0	2.9
Med-Mg alumina	3.24	21.9	73	0	1.5	2.1	1.6	0
Spinel	2.89	30.6	64.8	1.5	0	1.8	0.6	0.7
LoLo-Ca CaAl	1.29	5.3	66.9	6.2	4.9	16.7	0	0
Lo-Ca CaAl-Mg	3.32	13.6	42.7	1.3	4.2	33.3	3.1	1.8
Med-Ca CaAl	3.10	3.5	35.7	2.4	2.3	54.8	0	1.3
Med-Ca CaSAl	1.76	1.6	37.7	0.9	18.2	41.7	0	0
CaS	1.45	0	1.3	0	39.7	55.6	0	3.3

SEM Evaluation of Steel Samples

The SEM evaluations were performed using an ASPEX Instruments PSEM II microscope equipped with a Noran light element energy-dispersive spectrometer (EDS) detector. Individual inclusions were evaluated manually, but the bulk of the samples were evaluated using the automated feature analysis (AFA) option of the instrument. In this mode, predefined areas were scanned and every inclusion larger than 1.5 µm was detected and quantified. The location of each inclusion, size, area, composition, and its classification was recorded to a file, which could later be exported to Excel. The elements monitored during the SEM analysis included: magnesium, aluminum, silicon, sulfur, calcium, titanium and manganese. The composition of each inclusion was based on a normalized Kα ratio measurement of these elements. Each inclusion was classified based on its composition and predefined chemistry rules. Table 1 shows an example of typical inclusion compositions and their corresponding classification. Currently, more than 30 inclusion rules are used in the classification.

Table 2

Inclusion Compositions of Tundish Samples on the Same Heat to Verify the Reproducibility of the SEM Results

Tundish sample	T3	T4	T5	T6
% Mg	2.4	2.7	2.1	2.4
% Al	29.6	28.1	29.4	27.4
% Si	1.2	1.3	1.3	1.1
% S	15.5	16.3	15.3	16.7
% Ca	50.3	50.6	51.1	51.5
% Ti	0.6	0.5	0.5	0.5
% Mn	0.3	0.5	0.4	0.4
% Al/% Ca	0.59	0.55	0.58	0.53
# of inclusions	1,373	1,242	1,122	1,064
Inclusion index	27.9	26.4	30.2	29.0
Avg. size (µm)	3.0	3.1	3.4	3.4

An area of 5 x 10 mm that contains 128 scan fields was analyzed in each sample at a magnification of 250X. A number of experiments were conducted where bigger and smaller areas were analyzed, but it was determined that a 5 x 10 mm area gives the best balance between analysis speed and still being representative of the inclusions in the steel. Multiple tundish samples were taken 5 minutes apart in the latter part of a start-up heat to verify the reproducibility of the SEM analysis. The results from the verification study are shown in Table 2, which are weighted composition averages based on the size of the inclusions.

Typical inclusion results using the automatic feature analysis can be presented in table form, as shown in Table 2. However, a more visually appealing way to present the inclusion results is in the form of ternary composition plots, where three or more elements are selected and the composition of the inclusions is normalized based on the selected elements and plotted on the ternary diagram. The ternary plot in Figure 1 uses the elements Mg, Al and Ca and plots the compositions of the inclusions just after a heat was killed with Al. As expected, most of the inclusions plot close to the Al corner of the diagram. The ternary plot in Figure 2 uses the same elements but shows the inclusions at the end of desulfurization, where the inclusions now consist mostly of spinels. It is also very useful to plot the inclusions utilizing the elements Al, Ca and S, especially for heats that were over-treated with calcium or where the calcium was added at elevated sulfur levels. In Figure 3 (Mg, Al, Ca plot), the inclusions appear to be very Ca-rich calcium aluminates, but in Figure 4 (Al, Ca, S plot) it is clear that a large portion of the inclusions are actually CaS. Figures 3 and 4 are the ternary plots of sample T4 in Table 2.

While the ternary plots in Figures 1–4 are visually very informative, they do not always tell the whole story. Each dot in the ternary represents one inclusion and is given equal value regardless of the size. A more complete evaluation of inclusions has to take into account the

Figure 1

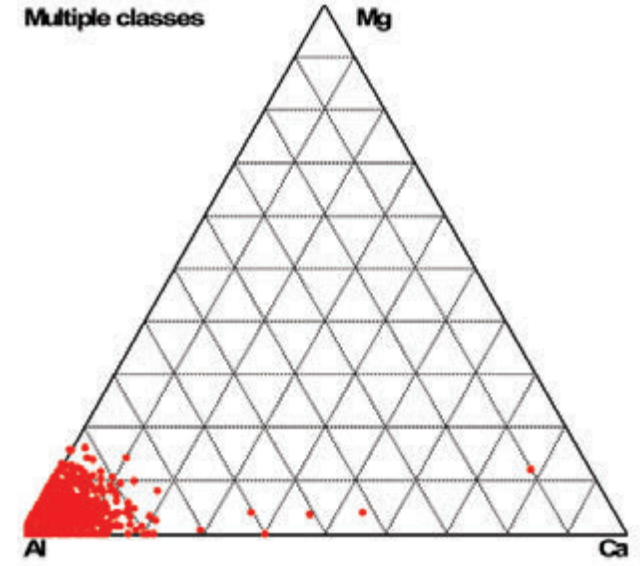

Ternary plot of inclusions just after Al addition.

Figure 2

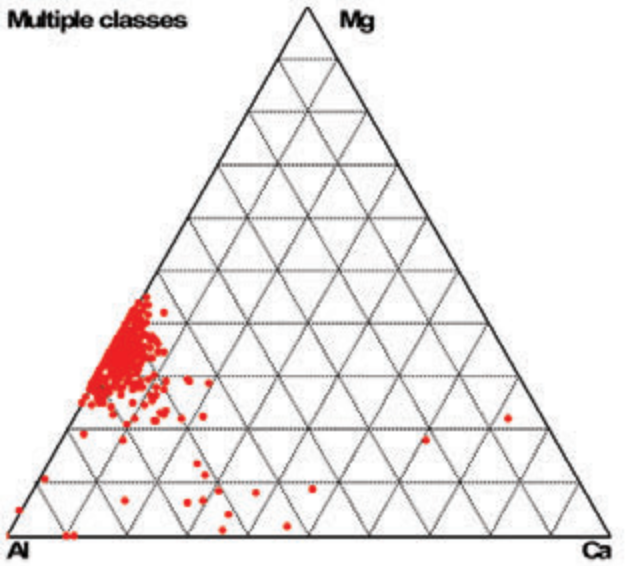

Ternary plot of inclusions after desulfurization.

size or area of the inclusions, and this is done with "area charts." Figure 5 is the area chart of the inclusions of sample T4 in Table 2.

Ternary plots and area charts, when combined, are excellent graphical tools to show why a heat clogged at the caster. Figures 6 and 7 show the ternary plot and area chart for the tundish sample from a heat that clogged at the caster.

The Mechanisms of Spinel Formation in Liquid Steel

In previous research, it has been proposed that spinels are formed from the interaction between low-oxygen steel and MgO-containing refractories,[9–11] arc-heating on slags at a ladle furnace,[12] as well as from alloys containing Mg. The typical Mg values in Al-containing materials are:

- Al cones: 0.01–0.8% Mg.
- Al wire: < 0.01% Mg.
- Al shred: 0.26–0.8% Mg.
- Al deox briquettes: 0.8–1.8% Mg.

The reaction of the Al antioxidants and carbon in the refractories and the Al in steel with the MgO in the refractories can lead to the following reactions (the [ ] denotes in solution in the steel, { } denotes in the refractories, and ( ) denotes in solution in the slag):

$$3\{MgO\} + 2[Al] = \{Al_2O_3\} + 3[Mg] \quad \text{(Eq. 1)}$$

Figure 3

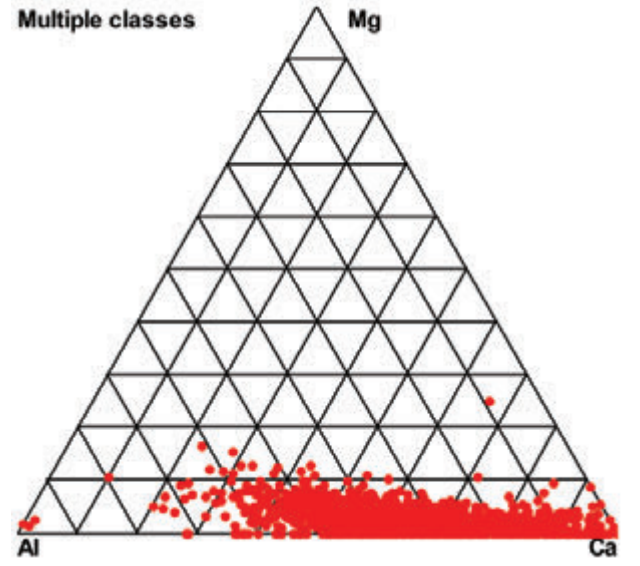

Ternary plot of inclusions of sample T4 (Table 2).

Figure 4

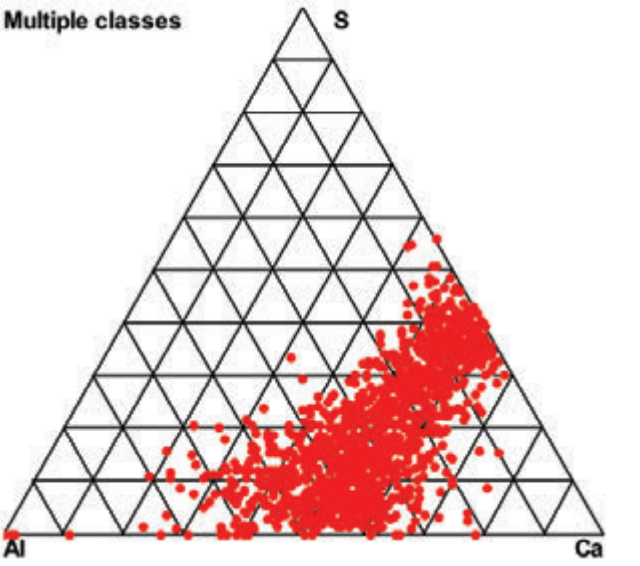

Ternary plot of inclusions of sample T4 (Table 2).

Figure 5

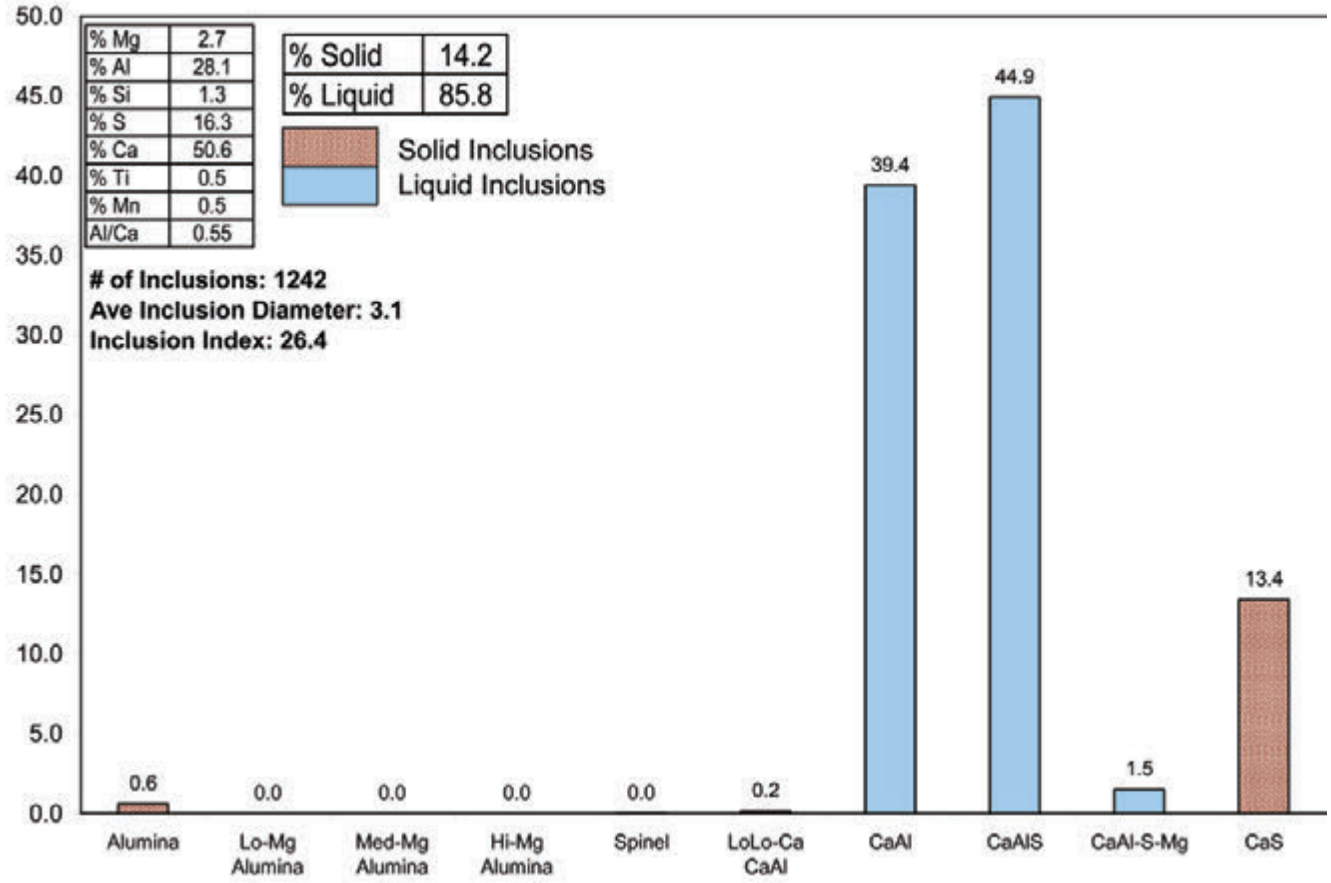

Area chart of the inclusion from sample T4 (Table 2). The y-axis presents the area % of the inclusions.

$$\{MgO\} + \{C\} = Mg(g) + CO \quad \text{(Eq. 2)}$$

Figure 6

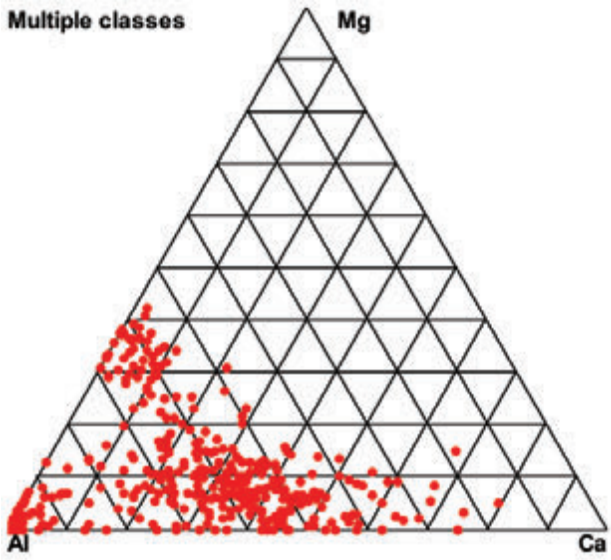

Ternary plot of inclusions of a heat that clogged at the caster.

$$Mg(g) = [Mg] \quad \text{(Eq. 3)}$$

While all these mechanisms are possible, in this paper it is proposed that the primary mechanism of spinel formation is via slag/metal interaction. Similar findings are reported in other studies.[3,6–8,13] In the production of low-carbon Al-killed (LCAK) steel via the EAF route, the steel tapped from the furnace contains significant levels of sulfur (typically > 0.025% S). The final sulfur requirement to cast LCAK steel in a CSP caster is typically < 0.008% S, so that extensive desulfurization is required at the ladle station. For effective desulfurization, the ladle slag is deoxidized with CaC_2 and Al-based deoxidizing agents until a light to white slag color is achieved. The %FeO + %MnO values in the slags are typically less than 0.7%. It is believed that the extensive mixing of the low-oxygen steel (< 6 ppm oxygen) with a well-deoxidized basic slag is the primary mechanism to form spinel inclusions in the steel.

The reaction of the slag with the added Al and CaC_2 for slag deoxidation can be written as follows:

$$3(MgO) + 2[Al] = (Al_2O_3) + 3[Mg] \quad \text{(Eq. 4)}$$

$$(MgO) + Ca = (CaO) + [Mg] \quad \text{(Eq. 5)}$$

Figure 7

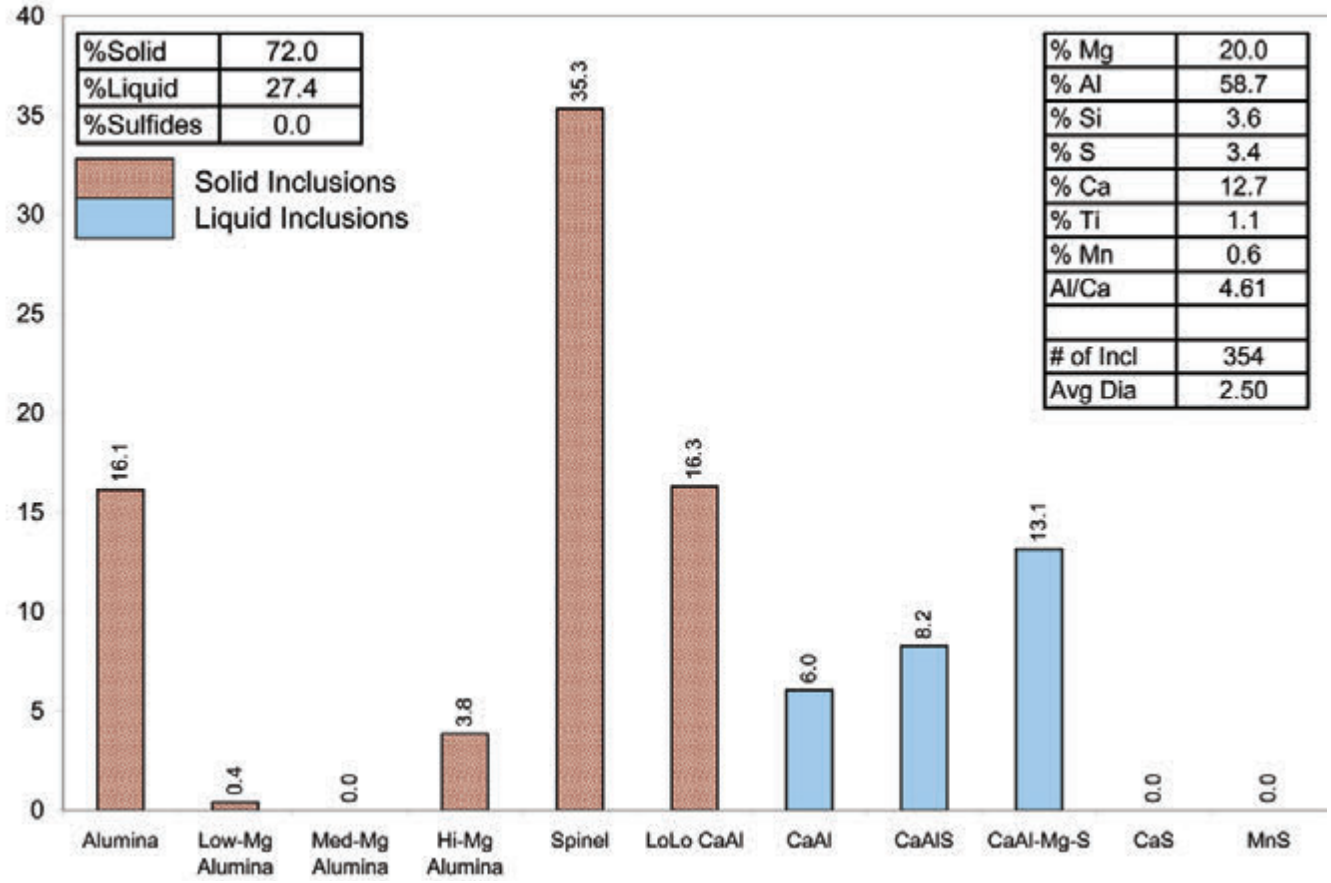

Area chart of inclusions of a heat that clogged at the caster. The y-axis presents the area % of the inclusions.

$$3[Mg] + 4Al_2O_3(incl) = 3MgAl_2O_4 + 2[Al] \quad \text{(Eq. 6)}$$

These reactions indicate that Mg in solution is required for spinels to form; this requires strongly reducing conditions and a source of Mg. These reactions are favored in basic well-deoxidized slag, and the Mg pickup increases as the slag basicity increases. There is still some discrepancy in the thermodynamic data for equilibrium solubility values of Mg and Al in liquid steel where spinel will be stable. Some indicate that spinel inclusions will form at Mg levels < 1 ppm for a typical 0.035% Al steel, whereas others indicate several ppms of Mg in solution before spinel will be stable.[13–17]

Table 3 shows the change in steel composition as a typical heat is processed at the LMF (L1 was taken at the beginning of the heat and L5 just before Ca treatment). The L1 sample (Al-containing sampler) represents the unkilled heat from the EAF. For the other samples in the table, "no-kill" samplers were used (containing no Al or Zr). Noteworthy is the increase in the Si level of the steel as the steel is desulfurized. No Si is added to the heat, so that the pickup in Si is a reflection of the oxidation state of the slag as SiO_2 in the EAF carryover slag is reduced. The slag is usually deoxidized using CaC_2 and/or Al-based materials.

Figures 8–11 are the ternary plots of the inclusions of these samples and show the change from alumina inclusions just after the steel was killed, to Mg-containing inclusions as the steel is desulfurized with a basic deoxidized slag.

Table 4 shows the change in inclusion composition for these four samples as the heat is processed at the LMF.

Figure 12 shows the relationship between the Si content in the steel and the Mg content of the inclusions

Table 3

Change in Steel Composition as a Heat is Processed at the LMF

Sample	%C	%Mn	%P	%S	%Si	%Al	%Ca
L1	0.028	0.033	0.008	0.032	0.000	(0.200)	0.0002
L2	0.044	0.250	0.010	0.026	0.011	0.042	0.0008
L3	0.044	0.248	0.010	0.016	0.015	0.048	0.0002
L4	0.045	0.247	0.010	0.011	0.017	0.050	0.0002
L5	0.047	0.253	0.010	0.007	0.022	0.045	0.0002

Figure 8

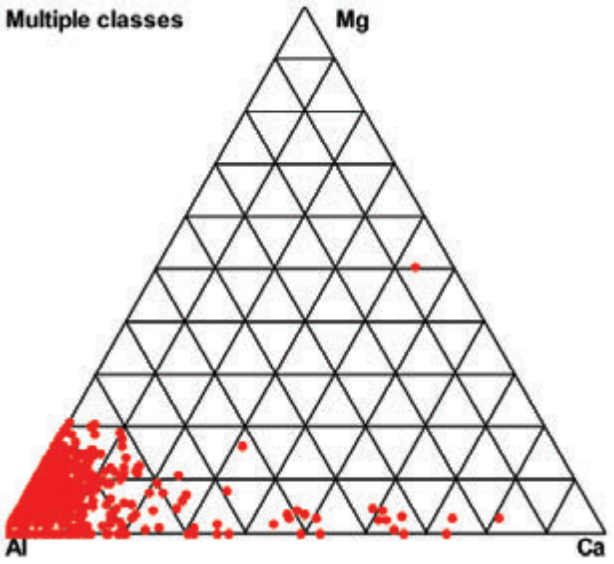

Ternary plot of inclusions of sample L2 (Table 3).

Figure 9

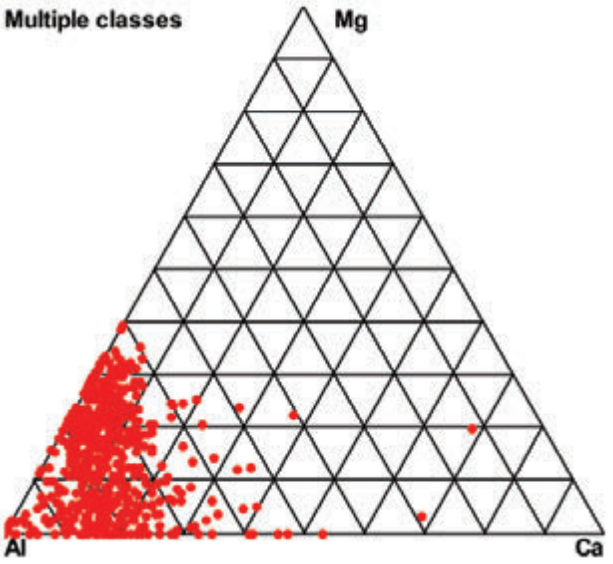

Ternary plot of inclusions of sample L3 (Table 3).

for a number of heats with similar amounts of EAF carryover slag. The more aggressively the slag is deoxidized, the higher the Si content in the steel and hence the higher Mg content in the inclusions. This figure offers further support that the mechanism of spinel formation in this study is via slag/metal interactions.

Phase Relations in the CaO-Al_2O_3-MgO System

It is an established practice to modify alumina (Al_2O_3) inclusions by Ca treatment. The solid Al_2O_3 inclusions are converted into liquid Ca-aluminate inclusions when sufficient amounts of Ca are added. The two key equations are:

$$xCa + (y + 1/3)Al_2O_3 = xCaOyAl_2O_3 + 2/3\ Al \quad \text{(Eq. 7)}$$

$$3CaO + 2Al + 3S = Al_2O_3 + 3CaS \quad \text{(Eq. 8)}$$

The added Ca can react with Al_2O_3 to form Ca-aluminates or with S to form CaS, or react with both. The modification of Al_2O_3 inclusions with Ca is typically displayed on the binary CaO-Al_2O_3 phase diagram. However, since the inclusions in this study contain significant amounts of MgO, the system CaO-Al_2O_3-MgO would be more representative. Figure 12 shows the 1,600°C (2,912°F) isothermal section of the CaO-Al_2O_3-MgO system as generated using the FactSage Software

Figure 10

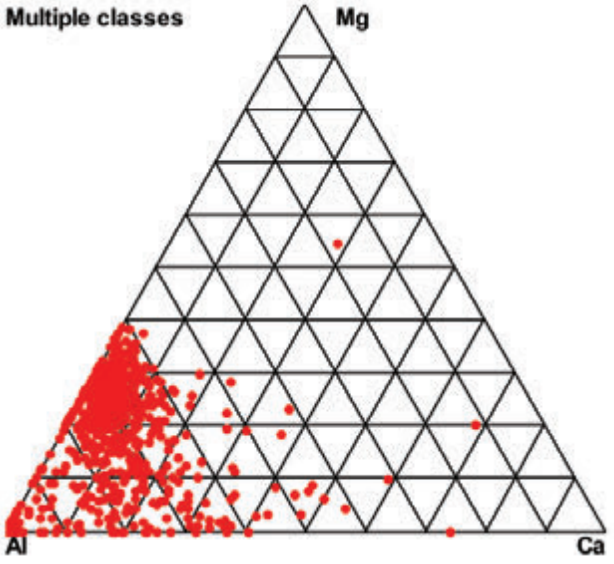

Ternary plot of inclusions of sample L4 (Table 3).

Figure 11

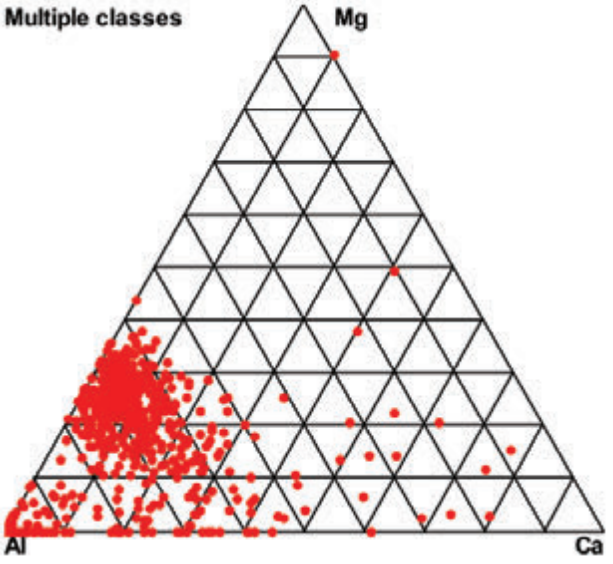

Ternary plot of inclusions of sample L5 (Table 3).

Figure 12

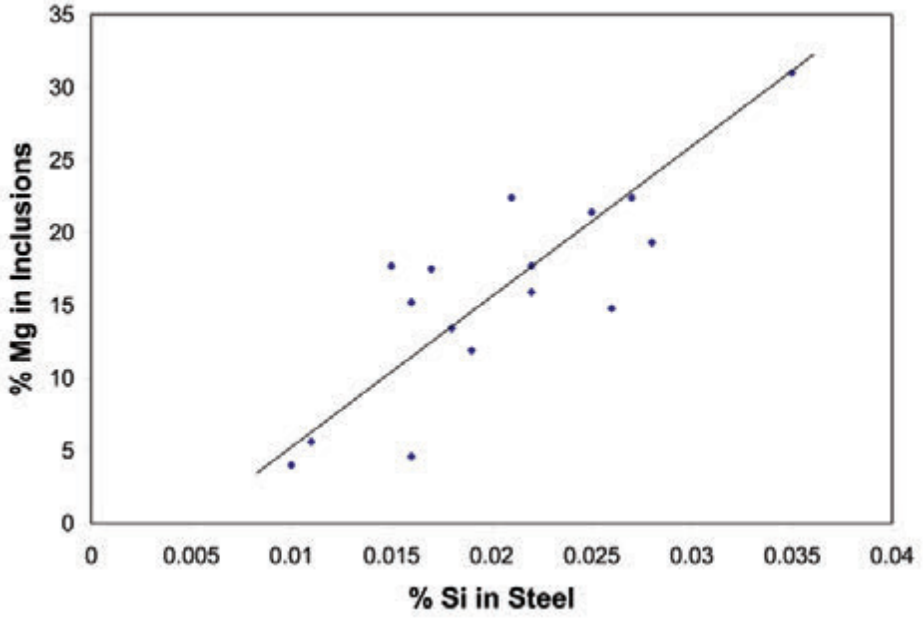

Relationship between the Si content in the steel and the Mg content in the inclusions before Ca treatment.

(Version 5.4). This figure shows the strong fluxing effect of MgO on Al_2O_3-CaO mixtures, whereby the all-liquid and liquid + solid regions widen appreciably when MgO is added.[3,8] Figure 13 also shows that there is some solubility of Al_2O_3 in spinel, so that the spinel composition (line c–e) ranges from about 17% MgO-83% Al_2O_3 to 26% MgO-74% Al_2O_3 ($MgAl_2O_4$). The line labeled a–b in Figure 13 shows the modification path of pure Al_2O_3 inclusions into the all-liquid area. The line c–d shows a potential modification path of the pure $MgAl_2O_4$ spinel inclusions by Ca. What is striking in this diagram is that 21% CaO would be required before an Al_2O_3 inclusion is modified into a liquid Ca-aluminate or the first liquid phase appears. In contrast, when CaO is added to spinel (c–d), a liquid phase forms immediately. This is graphically shown in Figure 14. These diagrams indicate that, from a strictly fundamental phase relation perspective, pure spinel ($MgAl_2O_4$) could be modified to form liquid inclusions, but not completely liquid inclusions. Furthermore, the reaction of CaO with spinel to form a liquid phase at low CaO levels suggests that spinel inclusions might be easier to modify than Al_2O_3 inclusions because of the faster ion transfer through a liquid boundary layer.

A number of studies have indicated that complete modification to 100% liquid inclusions might not be required for good castability. Good castability can be achieved even with a portion of the inclusions being either solid or semi-solid.[6,8,18] Pistorius et al.[8] suggest that clogging could be avoided if the inclusions contain more than 50% liquid, whereas Fuhr et al.[6] suggest that castability problems become more evident when the proportion of solid inclusions is higher than 60–70%. The tolerance for solid inclusions would certainly depend on the type of caster and the type of inclusions (alumina versus spinel).

While casting without significant clogging is possible with a mixture of solid and liquid inclusions, quality could be compromised. Slivers and laminations are sometimes observed in the heats with incomplete

Table 4

Inclusion Compositions for Sequential Samples on a Heat at the LMF

Sample	L2	L3	L4	L5
%Mg	5.6	17.7	17.5	17.7
%Al	58.5	59.2	66.0	59.2
%Si	2.8	3.9	2.8	3.9
%S	4.5	4.9	3.7	4.9
%Ca	26.4	11.8	8.3	11.8
%Ti	0.4	0.9	0.6	0.9
%Mn	1.7	1.7	1.1	1.7
Al/Ca	2.2	5.0	7.9	5.0
# of inclusions	563	566	591	587
Avg. size	7.8	3.2	3.1	4.1

Figure 13

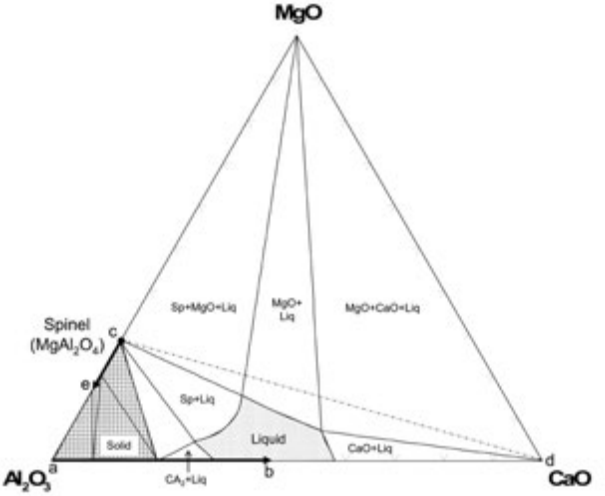

The 1,600°C (2,912°F) isothermal section through the CaO-Al_2O_3-MgO system.

Figure 14

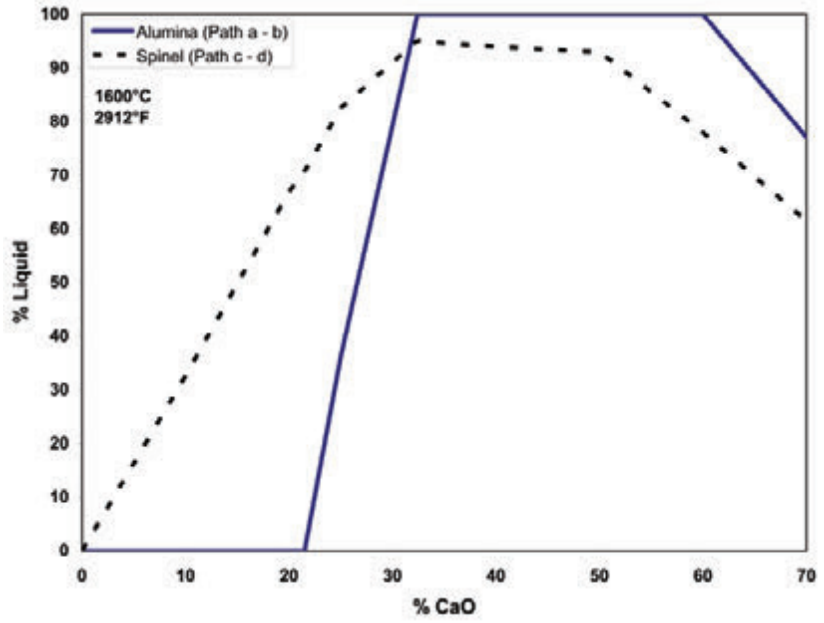

The amount of liquid that will form when CaO is added to alumina and spinel inclusions at 1,600°C (2,912°F).

inclusion modification. Both the chemistry and overall volume of inclusions are important.

Thermodynamic Considerations and the Modification of Spinel Inclusions With Calcium

The reaction of Ca with spinel inclusions can be written as follows:

$$Ca + (x + 1/3)[Al_2O_3 \cdot yMgO] = CaO \cdot xAl_2O_3 \cdot y(x + 1/3)MgO + 2/3\ Al \quad \text{(Eq. 9)}$$

or

$$Ca + MgAl_2O_4 = CaO \cdot Al_2O_3 + Mg,\ Mg = [Mg]\ and\ Mg(g) \quad \text{(Eq. 10)}$$

Equation 9 was originally proposed by Kor for the modification of spinel by Ca.[5] This reaction implies that the Al_2O_3 component of the spinel ($MgO \cdot Al_2O_3$) would be preferentially reduced by Ca. Equation 10 is an alternative expression, suggesting that the MgO component would be preferentially reduced by Ca. Conducting a detailed Gibbs free-energy evaluation for these two equations is possible, but the results would be dependent on the thermodynamic data source.[2,14–17] Instead, two thermodynamic software packages were used to calculate the possible modification of spinel inclusions by Ca treatment utilizing its free-energy minimization routines. The results of these calculations using the FactSage software (Version 5.4) and CSIRO's MPE32 (Version 3.2) package equipped with the Thermo-Calc engine are shown in Table 5.

The results in Table 5 show similar amounts of Mg in solution in the steel in equilibrium with spinel using

Table 5

Simulation of Spinel Modification by Calcium Using the MPE32 Software and FactSage Software

Steel composition	Initial conditions	MPE32 before Ca	MPE32 after Ca	FactSage before Ca	FactSage after Ca
%Al	0.035	0.0344	0.0344	0.0346	0.0349
%C	0.05	0.05	0.05	0.05	0.05
%Mn	0.25	0.25	0.25	0.25	0.25
%O (ppm)	10	3.3	0.8	2.35	1.12
%Mg (ppm)	5	2.52	4.94	3.21	4.74
%Ca (ppm)	0 (9)	0	0	0	0
%Fe	99	99.7	99.7	99.7	99.7
Inclusion type		Spinel	Liquid	Spinel	Liquid
Amount		0.00148	0.00245	0.00103	0.0008
%MgO		26	0.2	26	5.7
%Al_2O_3		74	48.4	74	46.2
%CaO			51.4		48.1
Gas phase (different units)					
Mg		2.52	4.94	0.108	0.302

Figure 15

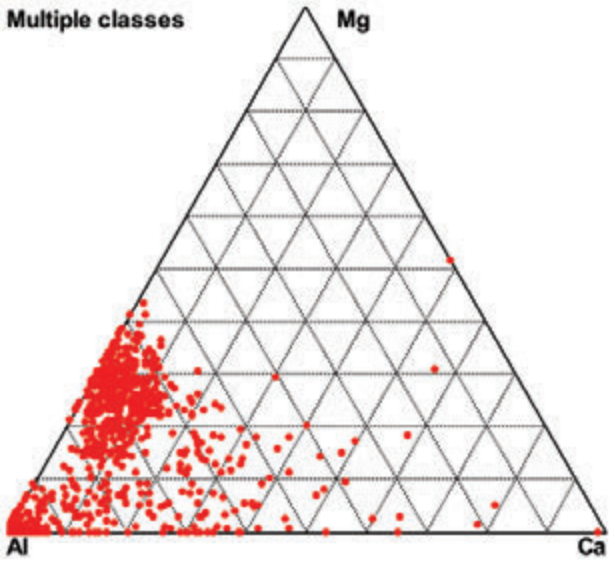

Ternary plot of inclusions of ladle sample before Ca.

Figure 16

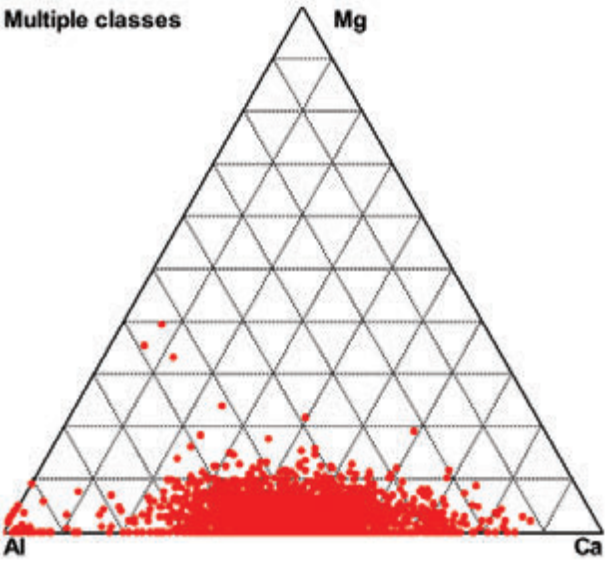

Ternary plot of inclusions of ladle sample after Ca.

the two models. Both models also agree that the spinel inclusions will be modified when sufficient amounts of Ca are added. The models consistently show a significant increase in the amount of Mg in solution after Ca addition, as well as an increase in the amount of Mg reporting to the gas phase. The oxygen potential in the steel is controlled by the Al/Al_2O_3 equilibrium, so that a decrease in the activity of Al_2O_3 in the inclusions ($^aAl_2O_3$) results in a decrease in the dissolved oxygen content in the steel. The increase in the Mg solubility (Table 5) is directly attributed to this decrease in dissolved oxygen content when the inclusions in the steel change from spinel ($^aAl_2O_3$ = 0.25) to liquid phase inclusions ($^aAl_2O_3$ = 0.027). These calculations suggest that, when Ca is added to spinel inclusions, they are modified to liquid inclusions, and that a portion of the MgO component in the spinel is reduced to Mg in the steel, and some report to the gas phase as Mg vapor that could be flushed out with the bubbles of Ar and Ca vapor. Since the reactions between liquid steel and inclusions approach equilibrium conditions because of extensive argon or electromagnetic stirring, it is believed that these calculations are useful to simulate spinel modification.

Figures 15–18, illustrating SEM inclusion results on steel samples, show that the modification of spinel inclusions with Ca actually occurs as predicted. The two examples presented here are representative of hundreds of samples, and the observed modification is consistent from heat to heat. Figure 15 shows the inclusions

Figure 17

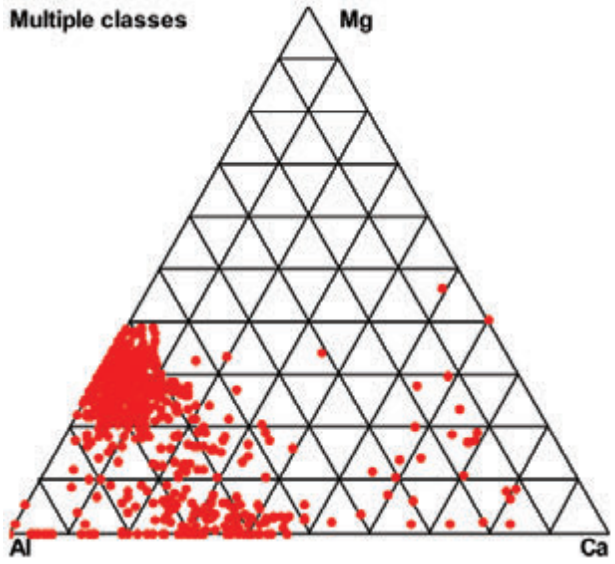

Ternary plot of inclusions of ladle sample before Ca.

Figure 18

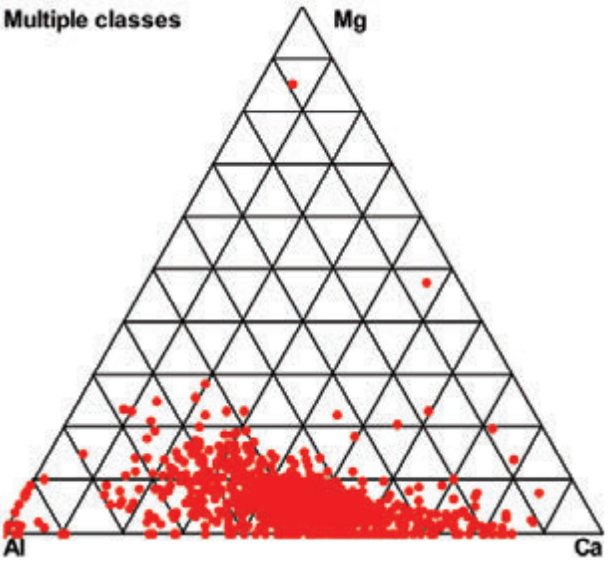

Ternary plot of inclusions of the caster (tundish) sample.

Figure 19

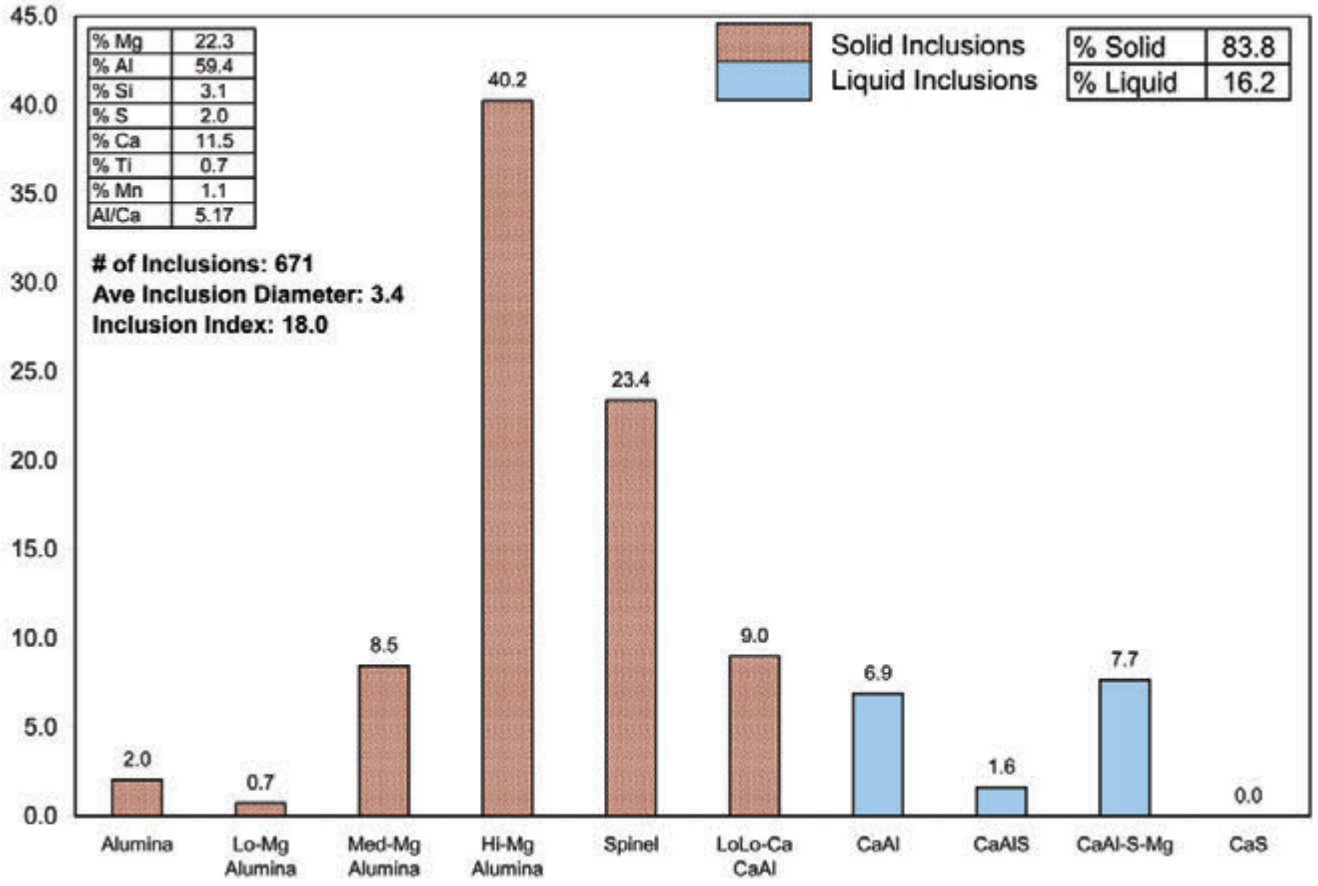

Area chart of inclusions in ladle sample before Ca treatment (Figure 17). The y-axis presents the area % of the inclusions.

in a heat at the LMF just before Ca addition, and Figure 16 shows the inclusions after Ca addition at the LMF. Figures 17 and 18 show the SEM inclusion results from another heat before and after Ca addition, respectively. Note that the results in Figure 18 represent the caster (tundish) sample.

The area charts for the samples in Figures 17 (before Ca) and 18 (tundish) are shown in Figures 19 and 20, respectively.

The averaged inclusion compositions in Figures 19 and 20 show the change in the Mg levels from before Ca treatment (22.3% Mg) to after Ca treatment in the tundish (5.8% Mg). The SEM results in these figures also show the increase in the number of inclusions from before Ca treatment in the LMF to after treatment at the caster. The liquid inclusions that form from spinel modification do contain some MgO so that there is a dynamic equilibrium between the Mg in solution and the MgO in the inclusions. However, at these levels, the residual MgO actually lowers the melting point of the inclusions and increases the composition range in the $CaO\text{-}Al_2O_3\text{-}MgO$ system for completely liquid inclusions (Figure 13).

Figure 21 shows the change in inclusion composition for a heat that was tracked from initial steel deoxidation, through desulfurization, before and after Ca treatment, at the caster and in the final strip. The L7 sample was taken directly after Ca treatment, and the L8 sample was taken at the LMF after a 5-minute post-Ca argon rinse.

The thermodynamic simulations (Table 5) indicated that the mechanism of spinel modification is the reduction of MgO by Ca to Mg into the steel, and to a lesser extent Mg vapor. The amount of Mg in all the inclusions before and after Ca addition was calculated for a number of heats by considering the compositions of the inclusions and the area fractions of the inclusions. Table 6 shows the change in the Mg amount in the inclusions before and after Ca additions for a number of heats.

The complete modification of spinel inclusion by Ca, and the decrease in the total Mg in Table 6, confirms that the mechanism of spinel modification occurs via the reduction of the MgO component of spinel to Mg into the steel and possibly to Mg vapor, which is carried out of the ladle together with the Ca vapor during Ca treatment.

In the initial phase diagram evaluation of spinel modification (Figure 13), it appeared that spinels could be modified to partially liquid inclusions, but that solid periclase (MgO) would be present as a phase with the liquid. In the hundreds of samples of the regular heats that were evaluated on the SEM, no MgO inclusions were observed. However, in a few isolated cases of solid MgO, inclusions were observed when the ladle slag had unusually high MgO levels due to the use of lime contaminated with dolomitic lime at the LMF.

In light of the data shown in Table 6, the path of spinel modification can be redrawn on the $CaO\text{-}Al_2O_3\text{-}MgO$ phase diagram as shown in Figure 22. The proposed path of spinel modification changed from c–d to c–f.

Figure 20

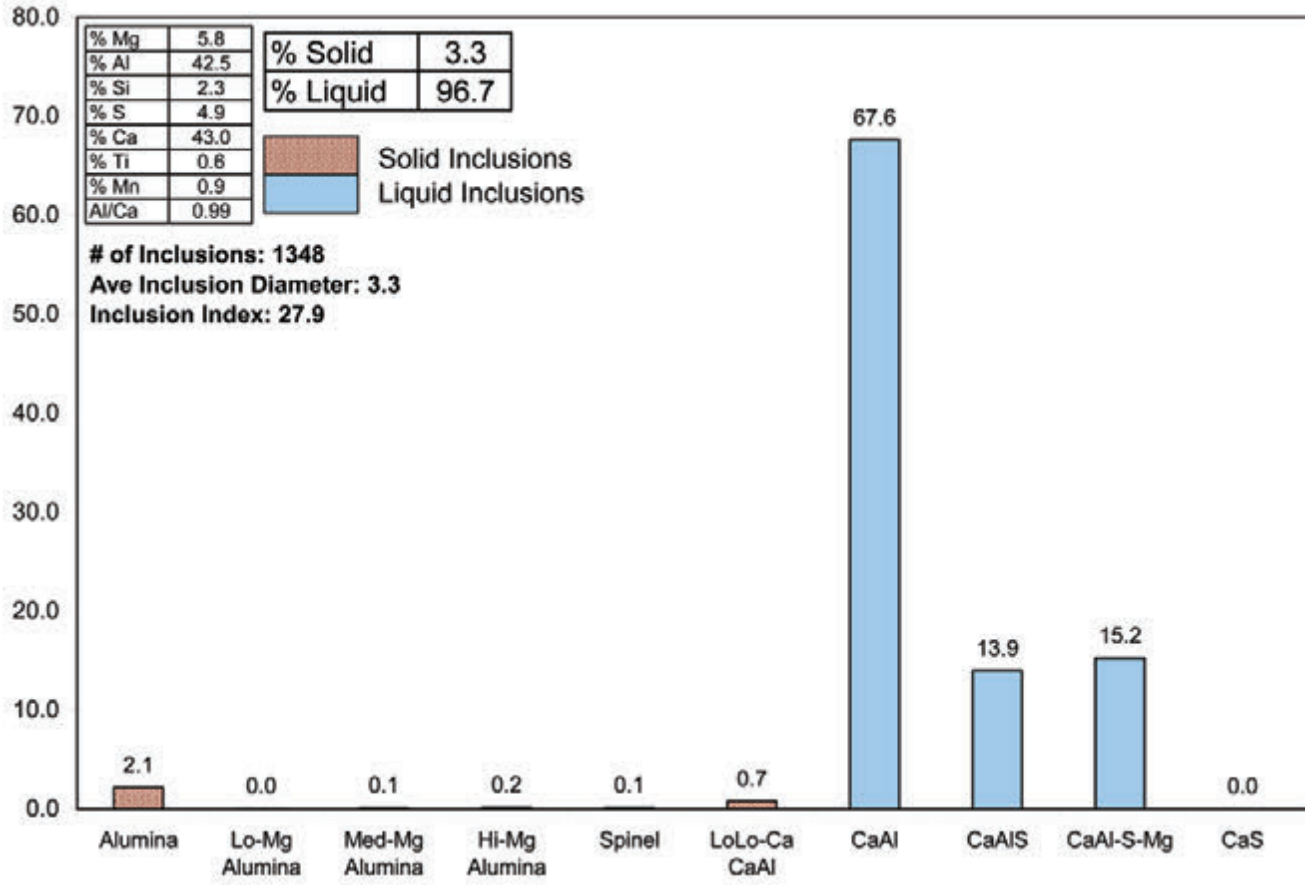

Area chart of inclusions in tundish sample (Figure 18). The y-axis presents the area % of the inclusions.

Figure 21

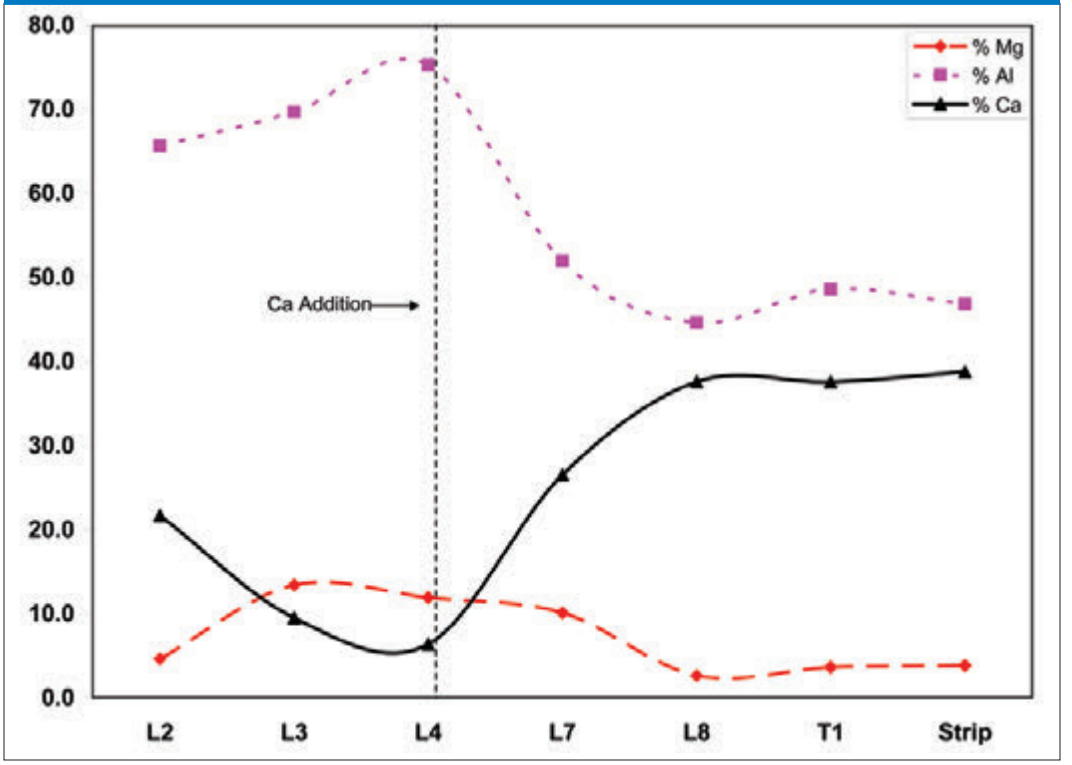

Change in inclusion composition (%) from steel deoxidation to final strip.

Table 6

Change in Mg Before and After Ca Treatment

	Total Mg before Ca	Total Mg after Ca	% change
Heat 1	1,175	471	60
Heat 2	1,763	1,044	41
Heat 3	812	533	34
Heat 4	1,385	1,040	25
Heat 5	976	706	28
Heat 6	577	284	51
Heat 7	819	503	39

The results thus far have clearly shown that spinel inclusions can be modified with calcium in LCAK steel. However, this does not imply that spinel inclusions can be modified in all grades of steel. The conditions in LCAK steel are very low oxygen potentials, which allow more Mg to go into solution during Ca treatment. In other steel grades with higher oxygen potential levels (Si-killed grades), the modification of spinel inclusions will probably not be possible, since the oxygen level in the steel is too high and there would be inclusions with components that are less stable than MgO (SiO_2 and MnO), which would rather react with the Ca so that the spinel inclusions would not be modified. For these grades of steel, the prevention or suppression of spinel inclusions should be pursued.[19–20]

Keeping the Spinels Modified

In the previous discussion, it was elucidated that the modification of spinel inclusion by Ca is accompanied by an increase in the amount of Mg in solution due to the decrease in oxygen potential in steel. It is therefore clear that any *increase* in the oxygen potential of the steel due to reoxidation could lead to *secondary* spinel formation. The oxidation state of the ladle slag is especially important before and during Ca treatment. It is believed that if the oxygen content of the steel is low (< 3 ppm O) and the Ca addition method is good, then all the *primary* spinel inclusions would be modified. However, if this steel is mixed during or after Ca treatment with a slag with a high oxygen potential (elevated FeO + MnO levels), secondary spinels could form as the Mg in solution encountered a higher oxidation potential environment. A second area for reoxidation of the steel and secondary spinel formation is at the caster, i.e., during start-up heats, ladle changes, and air ingress at joints during casting. Figures 23–26 show

Figure 22

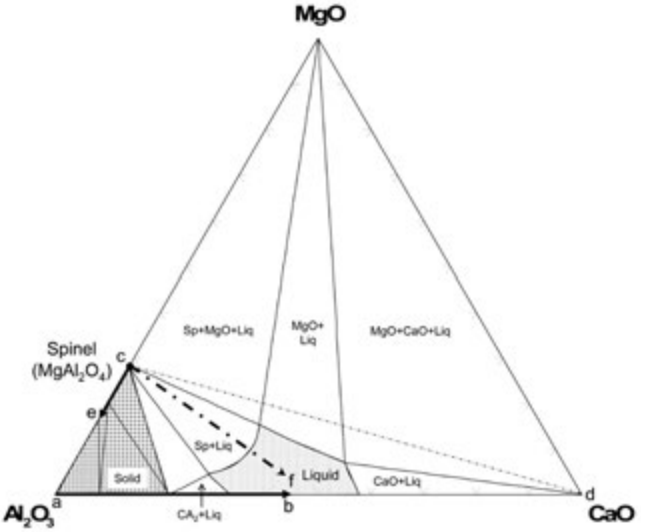

The 1,600°C (2,912°F) isothermal section through the $CaO\text{-}Al_2O_3\text{-}MgO$ system.

Figure 23

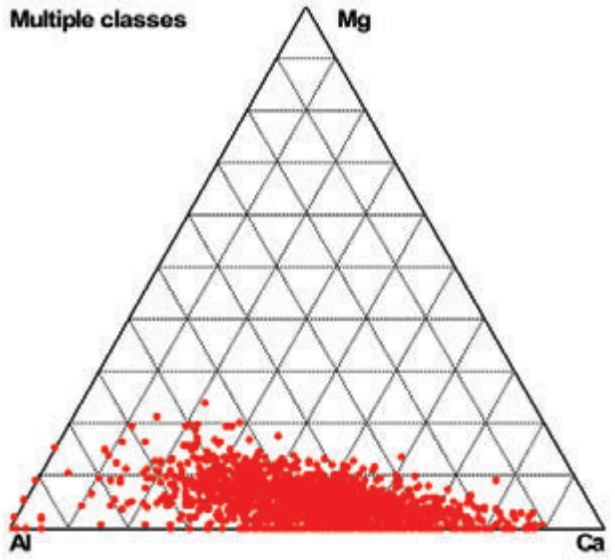

Ternary plot of inclusions of LMF depart sample.

Figure 24

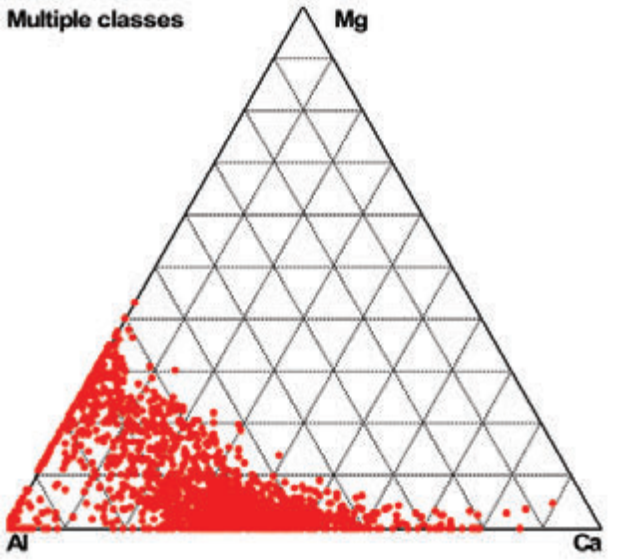

Ternary plot of inclusions of early tundish sample.

Figure 25

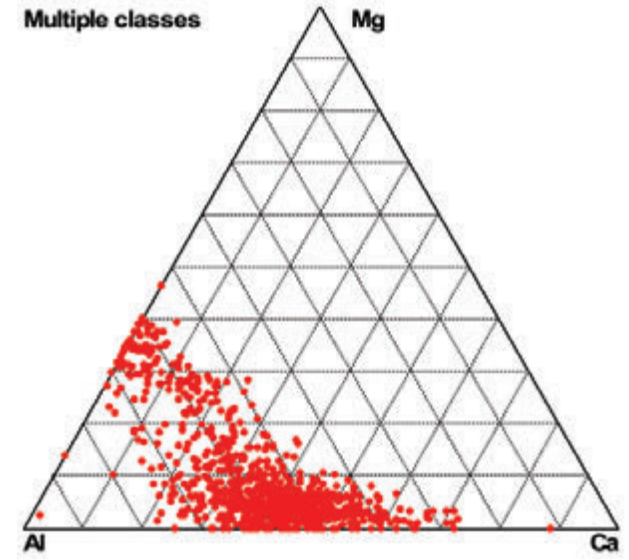

Ternary plot of inclusions of a strip sample taken from the beginning of the second slab.

Figure 26

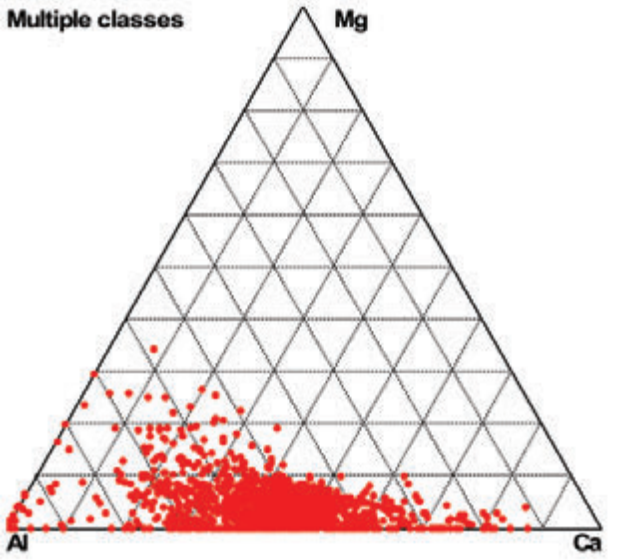

Ternary plot of inclusions of a tundish sample taken just after the stopper rod started to level out.

the change in inclusion composition at the beginning of a bad start-up heat where significant steel reoxidation occurred during start-up, to later in the cast when "fresh" well-shrouded steel entered the tundish. Figure 23 shows that the inclusions from the LMF depart sample are well-modified, with no spinels present. Figures 24 and 25 show a significant amount of *secondary* spinel, as well as alumina inclusions that form because of the reoxidation event early in the heat. Figure 24 presents a tundish sample, and Figure 25 represents a strip sample. In this particular heat, significant clogging occurred (stopper rod rise) at the beginning of the cast, but then stabilized as steel that was not exposed to oxygen entered the tundish. Figure 26 represents a tundish sample that was taken later in the heat just after the stopper rod started to level out.

Conclusions

This study is in agreement with other work that spinel inclusions can cause severe clogging at the caster. However, the data from this study shows that spinel inclusions can be effectively modified with Ca treatment. The presence of spinel inclusions is inevitable in the production of LCAK steel via the EAF route and CSP caster, since extensive desulfurization is required. It is believed that the spinel inclusions form by the extensive mixing of a low-oxygen steel with a well-deoxidized basic slag during the slag deoxidation and steel desulfurization step. It is proposed that the mechanism for spinel modification is the preferential reduction of the MgO component of spinel to Mg into solution in the steel. The residual Al_2O_3 from the spinel and resultant CaO react to form completely liquid inclusions. However, the increase of Mg in solution due to the lower oxygen potential after Ca treatment does make the steel more vulnerable to reoxidation and the formation of secondary spinel inclusions, which will also cause clogging. The effective modification of spinel inclusions requires low-oxygen-potential steel, well-deoxidized slags, and minimum reoxidation at the caster.

Acknowledgments

The initial work by Paretosh Misra (formerly of Nucor Steel–Berkeley) on spinel modification is acknowledged and appreciated. The technical input of Yves Vermeulen (Minteq) is also acknowledged. The authors would like to thank Ray Huffman for his assistance in preparing countless samples and running them on the SEM. The authors also wish to thank Nucor for allowing the publication of this work.

References

1. L.A. Frank, "Castability — From Alumina to Spinels (and More)," *Steelmaking Conference Proceedings,* ISS, 2001, pp. 403–416.

2. K. Fujii, T. Nagasaka and M. Hino, "Activities of the Constituents in Spinel Solid Solution and Free Energies of Formation of MgO, $MgO \cdot Al_2O_3$," *ISIJ International,* Vol. 40, No. 11, 2000, pp. 1059–1066.

3. B. Dekkers, B. Blanpain and P. Wollants, "Nozzle Plugging of Calcium-Treated Steel," *AIST Transactions, Iron & Steel Technology,* August 2004, pp. 92–98.

4. S-K. Jo, B. Song and S-H Kim, "Thermodynamics on the Formation of Spinel ($MgO \cdot Al_2O_3$) Inclusion in Liquid Iron Containing Chromium," *Met. Trans. B,* Vol. 33B, October 2002, pp. 703–709.

5. G.J.W. Kor, "Calcium Treatment of Steels for Castability," *First International Calcium Treatment Symposium,* Glasgow, Scotland, The Institute of Metals, 1988, pp. 39–44.

6. F. Fuhr, C. Cicutti and G. Walter, "Relationship Between Nozzle Deposits and Inclusion Composition in the Continuous Casting of Steels," *ISSTech 2003 Conference Proceedings,* 2003, pp. 165–175.

7. J.M.A. Geldenhuis and P.C. Pistorius, "Minimization of Calcium Additions to Low-Carbon Steel Grades," *Ironmaking and Steelmaking,* Vol. 26, No. 6, 2000, pp. 442–449.

8. P.C. Pistorius, P. Presoly and K.G. Tshilombo, "Magnesium: Origin and Role in Calcium-Treated Inclusions," *International Sohn Symposium,* TMS, 2006, pp. 373–378.

9. W. Loscher, W. Fix and A. Pfeiffer, "Reoxidation of Al-Killed Steels by MgO-Containing Basic Refractories," *ScanInject V,* Part IV, 1989, pp. 395–408.

10. V. Brabie, "Mechanism of Reaction Between Refractory Materials and Aluminum Deoxidized Molten Steel," *ISIJ International,* Vol. 36 Supplement, 1996, pp. S109–S112.

11. M. Boher, J. Lehmann and C. Gatellier, "An Experimental Study of Magnesium Transfer Between Tundish Refractory Lining and Liquid Steel, *Proceedings of UNITER'01,* Cancun, Mexico, 2004.

12. W. Tiekink, R. Boertje, R. Boom, R. Kooter and B. Deo, "Aspects of CaFe Cored Wire Injection Into Steel," *ISSTech 2003 Conference Proceedings,* 2003, pp. 157–164.

13. H. Todoroki, K. Mizuno, M. Noda and T. Tohge, "Formation Mechanism of Spinel-Type Inclusion in 304 Stainless Steel Deoxidized With Ferrosilicon Alloys," *Steelmaking Conference Proceedings,* ISS, 2001, pp. 331–341.

14. H. Itoh, M. Hino and S. Ban-Ya, "Thermodynamics on the Formation of Spinel Non-Metallic Inclusion in Liquid Steel," *Met. Trans. B,* Communications, Vol. 23B, 1997, pp. 953–956.

15. Y-B. Kang, C-H. Chang, S. Park, H. Kim, I. Jung and H. Lee, "Inclusion Control in Steels Containing Si, Mn, Ti, Mg and/or Al: Thermodynamic Prediction and Experimental Confirmation," *Metal Separation Technologies III,* 20–24 June 2004, Copper Mountain, Colo., USA.

16. W-G. Seo, W-H. Han, J-S. Kim and J-J. Pak, "Deoxidation Equilibria Among Mg, Al, and O in Liquid Iron in the Presence of $MgO \cdot Al_2O_3$ Spinel," *ISIJ International,* Vol. 43, No. 2, 2003, pp. 201–208.

17. D. Sichen, K. Beskow and T. Nagendra, "Formation and Chemical Development of Non-Metallic Inclusions in Steel in Ladle Treatment," *Metal Separation Technologies III,* 20–24 June 2004, Copper Mountain, Colo., USA. pp. 274–280.

18. A. Hamoen and W. Tiekink, "Are Liquid Inclusions Necessary to Improve Castability?" *Steelmaking Conference Proceedings,* 1999, pp. 229–233.

19. H. Gaye, C. Gatellier and P.V. Riboud, "Control of Endogenous Inclusions in Al-Killed and Low-Al Steels," *Turkdogan Symposium Proceedings,* 1994, pp. 113–124.

20. H. Gaye, C. Gatellier and J. Lehmann, "Fundamental Aspects of Slag Treatments in Secondary Steelmaking," *14th PTD Conference Proceedings,* 1995, pp. 53–58. ✦

This paper was presented at AISTech 2009 — The Iron & Steel Technology Conference and Exposition, St. Louis, Mo., and published in the Conference Proceedings.

Did You Know?

Roser Technologies Assists in AK Steel World Casting Record

Roser Technologies Inc. (RTI) played an integral role in the new world casting record set in May 2010 at AK Steel Middletown (see page 6 for details), by providing the advance mold coatings for 474,131 tons of continuously cast carbon steel. The record-breaking mold withstood 2,156 heats over 59 days, equivalent to 103 miles of carbon steel slab. Roser Technologies Inc., headquartered in Titusville, Pa., services all continuous casting molds for the AK Steel Middletown caster. The record-breaking mold had been equipped with narrowface coppers possessing TC1 spray coating and broadface coppers coated with TH nickel plating. These proprietary coatings have displayed tremendous success for many different casters and continue to break the barriers of conceivable mold life.

Founded by Daniel J. Roser in 2001, RTI has been working closely with AK Steel Middletown for nearly a decade to increase mold life and consequently decrease cost per ton and downtime. The extended life of one mold component requires advancements to several additional aspects of the rebuild process. The world-record continuous cast is the culmination of the joint efforts of RTI and AK Steel. In addition to coatings, RTI offers full-service engineering capabilities and state-of-the-art mold electronics capacity, as well as on-site mold inspection and installation.

The ownership, management and personnel of Roser Technologies Inc. are proud to be associated with AK Steel's new world record in casting. With each new technological accomplishment, new challenges are presented.

The double-strand caster at AK Steel's Middletown Works.

World Headquarters
Phone +1 503 726 7500

FEI Europe
Phone +31 40 23 56000

FEI Japan
Phone +81 3 3740 0970

FEI Asia
Phone +65 6272 0050

FEI Australia & New Zealand
Phone +61 3 9647 6200

Learn more at FEI.com

TÜV Certification for design, manufacture, installation, and support of focused ion- and electron-beam microscopes for the electronics, life sciences, materials science, and natural resources markets.